



**HAL**  
open science

## Sine Sweep Tracking Control of a Lightly-Damped Spacecraft

Samsul Arefin, Didier Dumur, Alain Bettachioli, Aurelien Hot, Sihem Tebbani

► **To cite this version:**

Samsul Arefin, Didier Dumur, Alain Bettachioli, Aurelien Hot, Sihem Tebbani. Sine Sweep Tracking Control of a Lightly-Damped Spacecraft. 24th International Conference on System Theory, Control and Computing (ICSTCC 2020), Oct 2020, Sinaia ( virtual ), Romania. pp.286-291, 10.1109/ICSTCC50638.2020.9259742 . hal-03034785

**HAL Id: hal-03034785**

**<https://hal.science/hal-03034785>**

Submitted on 1 Dec 2020

**HAL** is a multi-disciplinary open access archive for the deposit and dissemination of scientific research documents, whether they are published or not. The documents may come from teaching and research institutions in France or abroad, or from public or private research centers.

L'archive ouverte pluridisciplinaire **HAL**, est destinée au dépôt et à la diffusion de documents scientifiques de niveau recherche, publiés ou non, émanant des établissements d'enseignement et de recherche français ou étrangers, des laboratoires publics ou privés.

# Sine Sweep Tracking Control of a Lightly-Damped Spacecraft

Samsul Arefin

Université Paris-Saclay,  
CentraleSupélec, Laboratoire des  
signaux et systèmes,  
CNES,  
Department of Test, Simulation &  
Control, Thales Alenia Space  
Cannes, France  
samsul.arefin@centralesupelec.fr

Aurélien Hot

CNES, Structures and Mechanics  
Department  
Toulouse, France  
aurelien.hot@cnes.fr

Didier Dumur

Université Paris-Saclay, CNRS,  
CentraleSupélec, Laboratoire des  
signaux et systèmes,  
91190, Gif sur Yvette, France  
didier.dumur@centralesupelec.fr

Sihem Tebbani

Université Paris-Saclay, CNRS,  
CentraleSupélec, Laboratoire des  
signaux et systèmes,  
91190, Gif sur Yvette, France  
sihem.tebbani@centralesupelec.fr

Alain Bettacchioli

Department of Test, Simulation &  
Control  
Thales Alenia Space  
Cannes, France  
alain.bettacchioli@thalesaleniaspace.com

**Abstract**— Robust control of a lightly-damped system, such as the mechanical structure of a spacecraft, is a dilemma for control engineers. The shaker’s table used for satellite vibration tests for qualification uses a sine sweep acceleration signal to characterize the satellite’s frequency signature. The current control system presents strong oscillation while sweeping through high-frequency modes. Moreover, the process of fixing control parameters takes a long time leading to an increase in the testing costs. In this paper, a robust controller is proposed, based on an  $H_\infty$  synthesis. This approach reduces the duration of vibration testing, and eliminates the vibration for any sine sweep rate, for all lower and higher modes. Moreover, the proposed controller is able to achieve good stability margins, a certain level of delay margin, and a small tracking error, which complies entirely with the specifications.

**Keywords**—Sine sweep tracking, Vibration control, Lightly damped system,  $H_\infty$  controller

## I. INTRODUCTION

Among the tests required for the mechanical qualification of a satellite, sine tests on vibrator are used to confirm the mechanical resistance of structures and equipment, and thus to verify their resistance when excited by the launcher vibrations. Sine shake tests are usually performed in the aerospace industry to identify or assess the modal parameters of the satellite and compare them with the finite element model predictions. In order to perform these tests, a shaker’s table is commonly used to vibrate the satellite. The level of vibration, in this case, must be controlled so that the safety of the satellite is guaranteed. Therefore, this topic gives a vast insight into vibration control and robustness. Classically, vibration-related problems are solved with different methods based on the root locus plan, such as direct velocity feedback, positive position feedback, integral force feedback, etc. [7]. The main drawbacks of those methods are the lack of robustness, difficulty in treating unmodelled dynamics issues, and pole-zero flip-flops [7].

Consequently, more efficient control strategies are needed to achieve good behavior of the controlled system. In addition, in our case, vibration control concerns the problem of periodic tracking control while most of the researches of vibration testing deal with the disturbance rejection. Moreover, the vibration control deals with in general low-frequency signals, whereas, in our case, the signal considered is in a range from

low to high frequencies (between 5 to 150 Hz). In this frequency band, several satellite modes are located from low frequency to higher frequency. Therefore, the shaker control has to deal with all these modes. The main difficulty is related to the uncertain knowledge of the damping factor, damping ratio, and the existence of time delays. Consequently, advanced control strategies are needed to address this problem of frequency band sine sweep tracking for satellite tests.

A first approach was proposed based on an adaptive controller for regulating a sine signal [4]. This controller has issues like the beating phenomena that appear during the test when two modes are very close [5]. Even the higher sine sweep rate brings this oscillation as the system stays permanently in the transitional mode [5]. It can also happen because of the crosstalk among axes. In addition, the adaptive controller requires tuning parameters that are calibrated during a first test. This whole process takes a long time and is expensive. In addition, due to the uncertainty of the damping factor for the different tested signals, the tuned control parameters can lead to a significant overshoot from a testing run to another [4]. A second approach was proposed, based on an LQG controller [6]. This control strategy shows very promising results where the reference tracking is achieved accurately without any overshoot and/or undershoot [6]. However, this strategy does not allow any possibility to acquire robustness against the damping factor, damping ratio, or time delay. Moreover, there is no practical way to choose the tuning parameters of the LQG controller.

The first use of robust control strategy, such as  $\mu$ -synthesis for the multimode vibration control, has been successful in a disturbance rejection problem, resulting in the reduction of conservatism as well as the gain of robustness [8]. However, the previous controllers use nonlinear modeling of the system, especially for the reference signal. In this paper, a new control structure is proposed so that linear control strategies could be used. In particular,  $H_\infty$  control strategy will be applied for the considered control problem. The aim is to develop a controller that guarantees good performances as well as robustness with respect to model uncertainties.

The paper is organized as follows. In section II, the studied system is presented as well as the currently implemented adaptive controller. Section III defines the specification for control synthesis and focuses on the proposed control strategy

with the developments of the  $H_\infty$  controller design. Some simulation results are provided in Section IV. Finally, the conclusion and perspectives conclude the paper.

## II. DESCRIPTION OF THE SYSTEM

### A. Vibration test description

The vibration testing system is illustrated by Fig. 1. It includes an electromagnetic actuator producing the vibrations, linked to a table called shaker's table. The satellite is fixed on this table. A series of accelerometer sensors, called notch sensors, is fixed to the satellite in order to measure its acceleration and protect the hardware. Another series of sensors is fixed to the shaker's table to measure the input acceleration. When the shaker's input frequency goes through the satellite's vibration modes, the satellite starts to vibrate and some overshoots of hardware qualification status may occur. In this case, notch sensors are mainly used to decrease the input level and thus to control the satellite vibration and keep it under a safe limit. This measurement is then filtered by a high pass filter with a cutoff frequency of 0.5 Hz. From this filtered value, the maximum value of the magnitude of each sinusoidal period is estimated. Then, this value is compared with the reference, and the control block computes the necessary correction to reach the desired amplitude. This corrected value goes through an amplifier to power the actuator. Moreover, a user interface allows fixing the necessary control parameters and the reference.

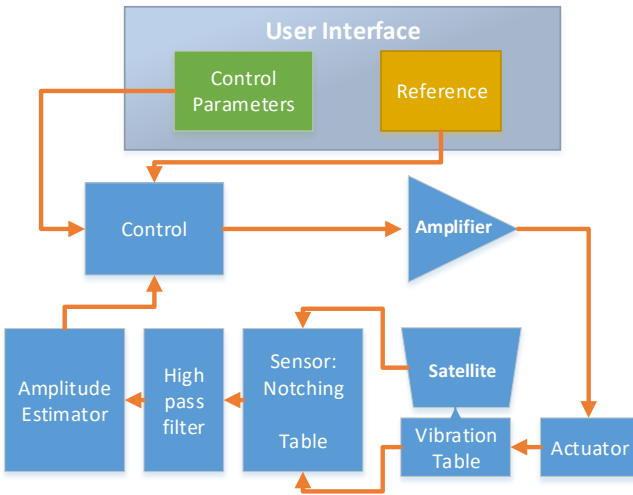


Figure 1. Vibration testing system

As previously mentioned, a frequency sweep is applied to the satellite in order to evaluate its frequency domain behavior and its resistance when excited by the launcher's vibration. The sweep rate is calculated so that the satellite undergoes the correct loads' duration of all the launcher spectrum, generally from 5 Hz to 150 Hz, without remaining too long on a resonant mode frequency.

The whole process of the vibration test goes through four steps, each step corresponding to a given input level on the table, in terms of acceleration magnitude: (i) very low level (0.125 g), this step is conducted to calibrate all control and system parameters as it is quite safe due to the low amplitude; (ii) low level (0.5 g); (iii) intermediate level (1 g) and (iv) qualification level (generally 2 g).

### B. Reference generation

The reference has two separate parts. The first part corresponds to its magnitude while the second one is the unit pseudo periodic sinusoidal signal sweeping from an initial frequency  $f_0$  to a maximal frequency  $f_{max}$ , called COLA (Constant Output Level Adaptor). This sine sweep acceleration signal can be characterized by its initial frequency  $f_0$  and the sweep rate  $\alpha$  (the speed of the frequency increase) [2]. Signal  $cola(t)$  is given by:

$$cola(t) = \sin(2\pi \frac{f_0}{\alpha} (e^{\alpha t} - 1) + \varphi_0) \quad (1)$$

where  $t \in [0, t_{max}]$  is the time,  $t_{max}$  the total test time,  $\varphi_0$  the initial phase.

In the real system, we also need to define the duration of the test  $t_{max}$ , which is a function of the maximal frequency  $f_{max}$ , as follows:

$$t_{max} = \frac{1}{\alpha} \log(\frac{f_{max}}{f_0}) \quad (2)$$

In order to simulate the current system, the definition of the duration  $t_K$  of each pseudo period  $K$  and its frequency  $f_K$  is also needed.  $t_K$  is approached by:

$$t_K = \frac{1}{\alpha} \log(1 + \frac{\alpha K}{f_0}) \quad (3)$$

while  $f_K$  is obtained from  $t_K$ :

$$f_K = \frac{1}{t_K} \quad (4)$$

Fig. 2 shows a typical example of a cola reference signal, generated with 1g magnitude, starting from 1 Hz and ending at 6 Hz, with a sweep rate of 20 octave/min.

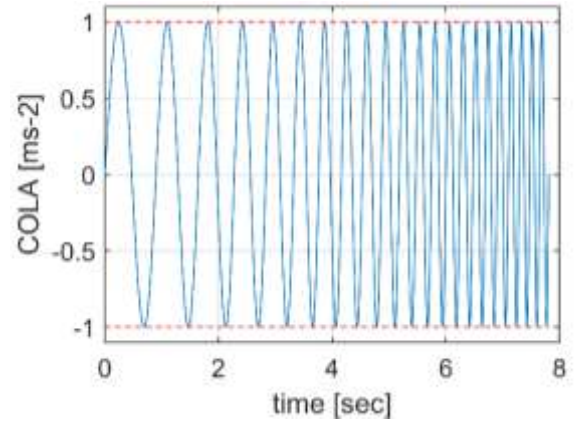


Figure 2. Example of a COLA reference signal

### C. Measurement and estimation

More than 600 accelerometers can be placed in different locations of the satellite and shakers table to measure the acceleration. The sampling frequency is between 6.4 kHz to 12.8 kHz. From the acceleration measurement, the maximum magnitude per pseudo period can be estimated as each period's timeline is known from the equation (4). Three methods, the maximal value, Root Mean Square or first harmonic approach, can be used to estimate this maximum value.

#### D. Current adaptive control strategy

The current closed-loop system is different from a classical feedback and feedforward control one [2]. It is represented in Fig. 3.

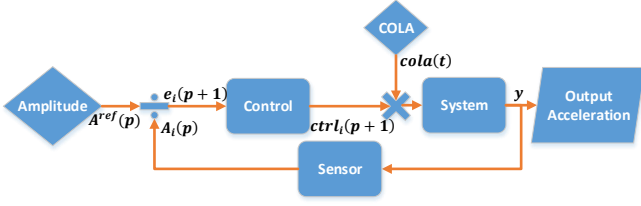


Figure 3. Current closed-loop vibration test

The tracking error is defined for this specific system as the ratio between the estimated magnitude and the reference issued from the  $i^{\text{th}}$  sensor among  $N$  sensors, given by:

$$e_{i \in [1, N]}(p+1) = \frac{A_{i \in [1, N]}(p)}{A_i^{\text{ref}}(p)} \quad (5)$$

where  $A_{i \in [1, N]}(p)$  is the estimated magnitude of  $i^{\text{th}}$  sensor over the  $p^{\text{th}}$  pseudo-period,  $A_i^{\text{ref}}(p)$  the reference magnitude for the  $p^{\text{th}}$  pseudo-period, and  $e_{i \in [1, N]}(p+1)$  the error of the  $i^{\text{th}}$  sensor taken into account at the  $(p+1)^{\text{th}}$  pseudo period.

The control signal  $ctrl$  is computed considering the minimum of all values  $ctrl_i$ ,  $i \in [1, N]$ , as stated by:

$$ctrl(p+1) = \min_{i \in [1, N]} (ctrl_i(p+1)) \quad (6)$$

where the  $ctrl_i$  signal is determined considering that the error is either higher than 1, or less than or equal to 1, according to the following equations [1]:

$$\begin{cases} ctrl_i(p+1) = ctrl(p) \frac{1+V}{e_i(p+1)+V} & \text{if } e_i > 1 \\ ctrl_i(p+1) = ctrl(p) \frac{1}{e_i(p+1)+V} & \text{if } e_i \leq 1 \end{cases} \quad (7)$$

The weight  $V$  is a tuning parameter, which determines the rapidity of the controller, given by:

$$V = \frac{40 \times (K_F - 1)}{T_{loop}} \quad (8)$$

where  $K_F$  is the compression factor, and  $T_{loop}$  is the time required to acquire and process the data.

Note that in (8),  $K_F = 1$  gives  $V = 0$ ; therefore, in this particular case, the control signal is simply given by:

$$ctrl(p+1) = \frac{ctrl(p)}{e(p+1)} \quad (9)$$

The error is in this case totally compensated at the next pseudo period. However, increasing  $K_F$  leads to an increase of  $V$  and a decrease of the control signal, meaning a slower response. In general, the  $K_F$  value remains in the range from 1 to 20.

Studying the stability of this controlled system is not an easy task since the control signal is elaborated through logical statements, on the one hand, and two sampling periods have to be considered on the other hand. Firstly, as illustrated in

Fig. 3, the sensor captures the acceleration value at a very high sampling frequency (from 6.4 kHz to 12.8 kHz). Then, as previously explained, the maximum magnitude value is estimated over each period. From this point, the sampling period is variable, which value is the one of the pseudo period. During this sampling period, the estimated maximum magnitude value is used to generate the control signal. Therefore, for each period, the control signal is computed only once. This signal is multiplied by the periodic signal  $cola(t)$  and the final control signal is again sampled at the sensor sampling frequency.

### III. PROPOSED $H_\infty$ CONTROL STRATEGY

#### A. Reformulation of the closed-loop system

To implement advanced linear control strategies, the current control scheme of Fig. 3 has to be reformulated under a standard control loop. The two parts of the reference signal need to be combined within a unique signal. The control structure is given in Fig. 4. The first benefit of this structure is that only one sampling frequency is used for the whole system (which can be selected from 6.4 kHz to 12.8 kHz). It will thus limit the error within a very small bound as the correction is done at each sampling period rather than during an entire pseudo period. Secondly, the stability margin could be determined in this case.

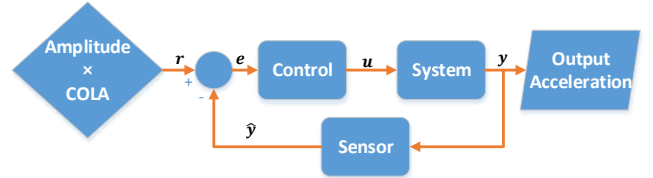


Figure 4. Adapted closed-loop system for robust control

#### B. Specifications for the design

The design of the controller must be carried out to fulfill the following specifications. The tracking error  $e$  must be in the range of  $\pm 5\%$ , the control effort must not exceed 75g, while keeping  $30^\circ$  phase margin and 6 dB gain margin in the frequency range 5 to 150 Hz. Within this frequency range, the estimator filters the signal, therefore no noise filtering specification needs to be added. Moreover, the controller has to be robust with respect to variations of system parameters.

#### C. $H_\infty$ controller design

##### 1) Formulation of the control problem

Consider the feedback structure of Fig. 5. Signals  $r(t)$ ,  $y(t)$ ,  $e(t)$ ,  $u(t)$ ,  $w_i(t)$ ,  $w_0(t)$ ,  $n(t)$  correspond to the reference, output acceleration, error, command, plant input disturbance, plant output disturbance, measurement noise, respectively.

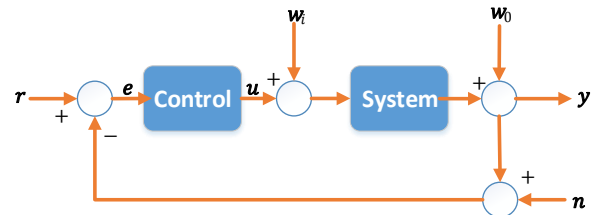


Figure 5. Feedback tracking control with noise and disturbance

Denoting  $G(s)$  the system transfer function and  $K(s)$  the controller, with  $s$  the Laplace variable, the following transfer functions can be defined:

- the sensitivity function which represents the transfer function between the reference  $r$  and the error  $e$ :

$$S(s) = (I + G(s)K(s))^{-1} \quad (10)$$

- the complementary sensitivity function which represents the influence of the noise on the system error:

$$T(s) = (I + G(s)K(s))^{-1}G(s)K(s) \quad (11)$$

- the sensitivity function on the command which represents the energy of the control signal  $u$ :

$$R(s) = K(s)(I + G(s)K(s))^{-1} \quad (12)$$

## 2) Weight selection

Frequency domain specifications can be directly imposed on sensitivity functions through an appropriate choice of weighting functions  $w_i$ , in order to satisfy the specifications mentioned in Section III.B [10]. These weighting functions are represented in Fig. 6 and introduced in the following equations considering the maximum singular values of the sensitivity functions:

$$\begin{cases} \bar{\sigma}(S(s)) < |w_1^{-1}(s)| \\ \bar{\sigma}(R(s)) < |w_2^{-1}(s)| \\ \bar{\sigma}(T(s)) < |w_3^{-1}(s)| \end{cases} \quad (13)$$

leading to:

$$\begin{cases} \bar{\sigma}(S(s)w_1(s)) < 1 \\ \bar{\sigma}(R(s)w_2(s)) < 1 \\ \bar{\sigma}(T(s)w_3(s)) < 1 \end{cases} \quad (14)$$

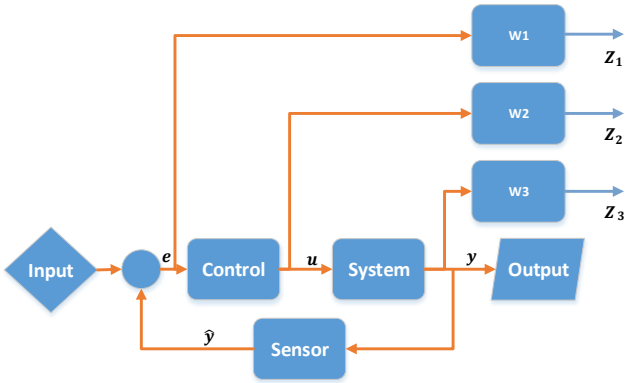


Figure 6. Weight definition for  $H_\infty$  control synthesis

The error signal can be minimized and the sensor noise rejected at the same time by constraining  $S(s)$  at low frequencies and  $T(s)$  at high frequencies, assuming that the sensors perform perfectly at low frequencies and will not introduce noise in the frequency band where the tracking error needs to be controlled. Therefore, the weighting functions  $w_i$  are determined to constraint  $S(s)$  and  $T(s)$ . The augmented model described in Fig. 6 is denoted by  $P$  and the standard linear fractional representation of  $P$  and  $K$  is denoted by  $F(P, K)$ . The computation of the  $H_\infty$  robust controller can be achieved by minimizing  $\|F(P, K)\|_\infty$ , over the set of all controllers  $K(s)$  which stabilize the internal states of the system. The minimum gain is called  $H_\infty$  optimal gain  $\gamma_{opt}$ . This can also be realized in a sub-optimal way, that is, for

$\gamma > 0$ , find the controller that stabilizes the internal states of the system and satisfies  $\|F(P, K)\|_\infty < \gamma$ . This approach will be further considered.

## IV. SIMULATION RESULTS

### A. Case study

In order to illustrate the control strategy, a simplified mechanical system with a single vibrating mode is considered, where the satellite is considered as a simple mass (single degree-of-freedom oscillator). The dynamical behavior of this system is governed by:

$$\ddot{x} + 2\xi\omega_n\dot{x} + \omega_n^2x = \frac{F_0}{m} \quad (15)$$

where  $x$  represents the displacement,  $\xi$  the damping factor,  $\omega_n$  the mode frequency,  $F_0$  the applied force, and  $m$  the mass. This equation can be rewritten in the space-state formalism with an input acceleration  $u = \frac{F_0}{m}$ :

$$\begin{cases} \begin{bmatrix} \dot{x} \\ \dot{x} \end{bmatrix} = \underbrace{\begin{bmatrix} 0 & 1 \\ -\omega_n^2 & -2\xi\omega_n \end{bmatrix}}_A \begin{bmatrix} x \\ \dot{x} \end{bmatrix} + \underbrace{\begin{bmatrix} 0 \\ 1 \end{bmatrix}}_B u \\ y = \underbrace{\begin{bmatrix} -\omega_n^2 & -2\xi\omega_n \end{bmatrix}}_C \begin{bmatrix} x \\ \dot{x} \end{bmatrix} + u \end{cases} \quad (16)$$

with  $y$  the output acceleration.

### B. Controller synthesis

Weighting functions can be selected either manually by understanding the specification of the closed-loop system or automatically. Some approaches in the literature explain a systematic way to achieve appropriate weight for a steady-state periodic tracking controller [9]. However, those approaches are mostly suitable for some specific problems. In our study, the weighting functions are obtained manually.

#### Weighting function $w_1$ :

Error requirements are used to define  $1/w_1$ . It is designed as a first-order high-pass filter with a magnitude of the accepted error chosen equal to 1%. The range of the test is between 5 to 150 Hz. So the corner frequency is set far from this range, at 450 Hz. The filter transfer function is given by:

$$w_1 = \frac{2827s + 7.994e10}{2827s + 7.994e6} \quad (17)$$

#### Weighting function $w_3$ :

The noise profile is used to define this weight. A first-order low pass filter is considered for  $1/w_3$  to let all signals pass through at low frequencies, but filter the high-frequency noise. The corner frequency is 700 Hz, which is higher than the selected corner frequency defined for the first weight.

$$w_3 = \frac{1.759e6s + 7.738e09}{1.759e4s + 3.095e10} \quad (18)$$

#### Weighting function $w_2$ :

This additional constraint is applied to limit the control signal below the saturation limit of the actuator. It is chosen here constant and its value is set to 0.02.

Fig. 7 shows the magnitude of  $\frac{1}{w_1}$  and  $\frac{1}{w_3}$  with respect to the angular frequency in rad/s.

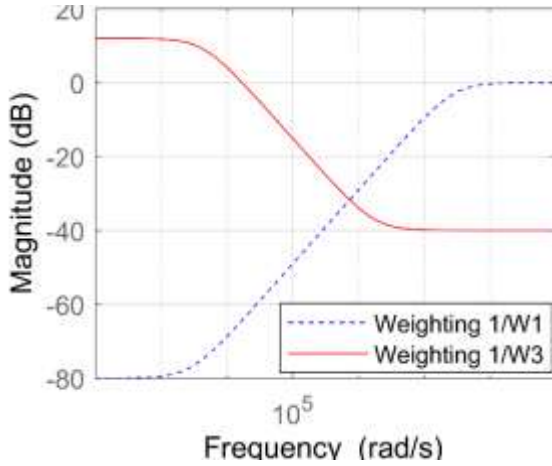


Figure 7: Weighting function  $\frac{1}{w_1}$  and  $\frac{1}{w_3}$

For the considered application, the controller has been designed with a mode at 15 Hz and 0.01 damping factor. Its transfer function is given by:

$$K(s) = \frac{2.8e5 s^3 + 4.9e11 s^2 + 9.3e11 s + 4.3e15}{s^4 + 7.5e5 s^3 + 2.9e9 s^2 + 2.3e12 s + 7.5e10} \quad (19)$$

### C. Frequency domain verification

The Nichols chart has been used to analyze the stability of open-loop controlled system (Fig. 8) where the input is the error signal  $e$  and the output is the measured acceleration  $\hat{y}$ . The designed controller provides an internally stabilized system with a phase margin of  $90^\circ$ , delay margin of 0.996 sec at 0.75 Hz. This system is infinitely stabilized in terms of gain.

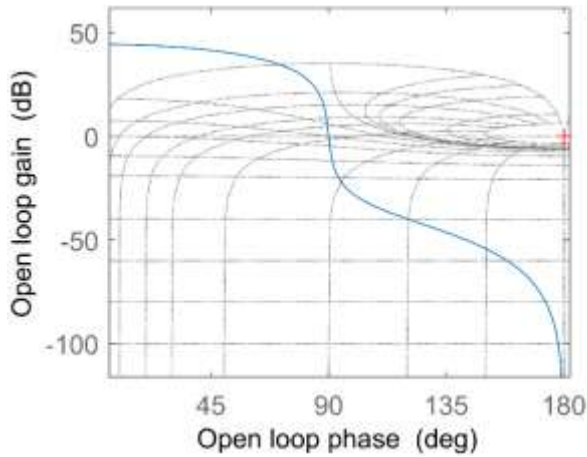


Figure 8. Nichols chart of the controller system (zoom with frequency range between 5 and 150 Hz)

### D. Time domain verification

In order to verify the improvement of the newly designed controller, two different time-domain simulations have been performed. Fig. 9 and Fig. 10 illustrate the result obtained with the current adaptive control strategy and with the  $H_\infty$  controller, respectively. The COLA signal is generated within the range of 5 to 30 Hz with a magnitude of 1 g. The

mode frequency is set at 15 Hz, corresponding to the first mode of a typical commercial geostationary satellite, and the damping factor is 1%.

#### 1) Current performance with the adaptive controller

The current adaptive controller's performance is demonstrated in Fig. 9 for a damping factor of 1%, a sine sweep rate of 3 octave/min and a compression factor of 20. This is more likely to be the case of a real satellite, a maximum compression factor of 20 cannot even keep the error below the specification, and very high oscillations are observed.

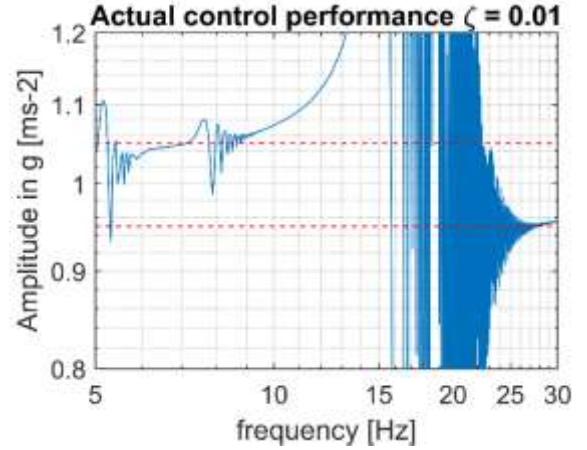


Figure 9. Output acceleration with current control strategy with compression factor

#### 2) $H_\infty$ controller performance

In this section, the performance of the  $H_\infty$  controller is discussed. In this case, the configuration is the same as the previous one, the damping factor is 1%, sweep rate is 3 octave/minute. Fig. 10 illustrates the obtained results.

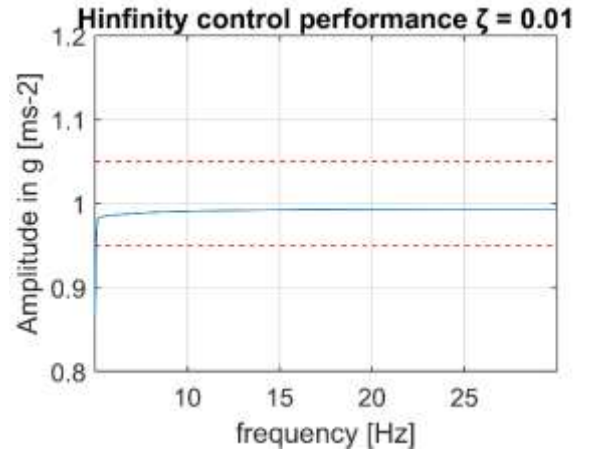


Figure 10. Output acceleration with  $H_\infty$  controller

The obtained tracking error remains below 5% and no oscillation at the neighborhood of the mode (15 Hz) is noticed. The change of sine sweep rate from 1 to 5 octave/min has so far no influence and introduces no oscillations at all.

Even though the obtained performance is noticeably good compared to the current strategy, the control effort must also be analyzed, as it should stay below the maximum capacity of the actuator. With the weighting value  $w_2$  described in section (III-B), the control effort is kept below 75g (Fig. 11).

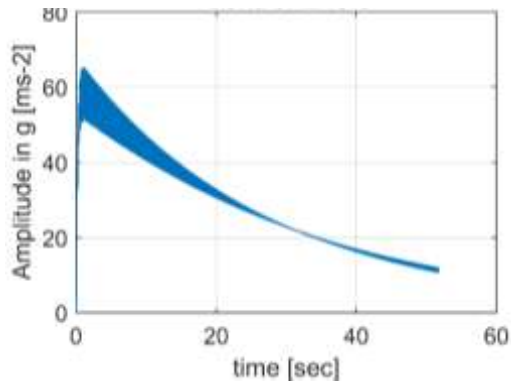


Figure 11. Control effort profile of the  $H_\infty$  controller

### 3) Robustness against time delay and damping factor

Some additional tests have been carried out to check the robustness of the proposed control strategy and are illustrated in Fig. 12 and Fig. 13. A first simulation considers the case where a one second time delay is introduced to the system dynamics (blue dots). It can be noticed that the system remains robust and tracks the reference signal, Fig. 12.

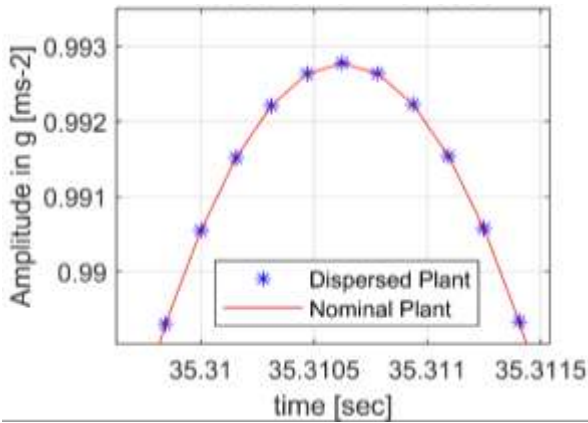


Figure 12. Robustness against delay zoomed over a period

In a second simulation, a mismatch of -15% on the damping factor is applied. The obtained result given in Fig. 13 (blue line) is compared to the nominal case (orange line).

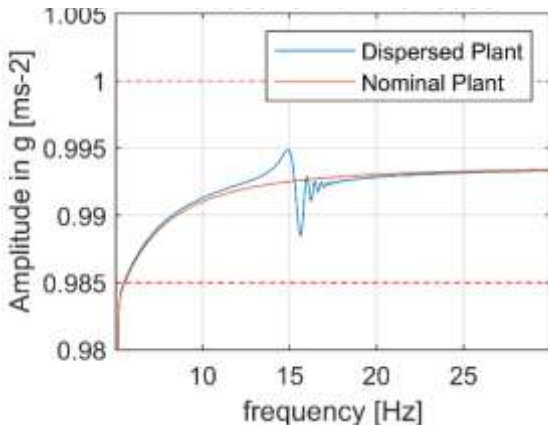


Figure 13. Robustness against the damping factor mismatch

The controller shows very good robustness against the variation of the damping factor with an error always below 2%.

## V. CONCLUSION

The main objective of this work is to eradicate the oscillations appearing during vibration tests as well as reducing the time of these vibration tests. The contribution of this work is mainly based on replacing the existing controller and introducing a new robust control strategy. Therefore, the  $H_\infty$  design method is considered, introducing weighting transfer functions that are directly linked to industrial specifications. The obtained performances are much better than those observed with the existing controller, based on the considered case of study. The proposed controller eliminates all types of vibration and is not dependent on parameters such as the compression factor as well as the sine sweep rate compared to the actual control strategy. Moreover, the error remains below 5% without saturating the actuator. Although the achieved result is far superior, the robustness test has not been done in the case of mode frequency variation and in case of the presence of several modes. Therefore, further research should be carried out to assess the robustness of the control strategy in the presence of parametric dispersions of the plant. In addition, the multi-vibrational modes system should be considered as real satellites have several modes.

## REFERENCES

- [1] J. Wijker, "Mechanical vibrations in spacecraft Design", Springer, 2004.
- [2] A Girard and N. Roy, "Structural dynamics in industry", ISTE Ltd and John Wiley & Sons, ISBN: 978-1-84821-004-2, 2008.
- [3] C. Lalanne, "Mechanical vibration & shock analysis", Vol 1: Sinusoidal Vibrations, 2nd Edition. John Wiley & Sons, 2009.
- [4] A. Bettacchioli, P. Nali, "Common issues in S/C sine vibration testing and a methodology to predict the sine test responses from very low level run," Proceedings of the 29<sup>th</sup> Aerospace Seminar, Los Angeles, October 2015.
- [5] A. Bettacchioli, P. Nali, "Beating Phenomena in spacecraft sine test and attempt to include sine sweep rate into the test prediction," Proceedings of the 13<sup>th</sup> European Conference on the Spacecraft Structure, Materials and Environmental Testing, Brunswick, April 2014.
- [6] A. Bettacchioli, "Feasibility study of the beating cancellation during the satellite vibration test," Proceedings of the 14<sup>th</sup> European Conference on the Spacecraft Structure, Materials and Environmental Testing, Toulouse, September 2016.
- [7] A. Preumont, "Vibration control of active structures: an introduction". Vol. 246. Springer, 2018.
- [8] G. Balas, "Robust control of flexible structures: theory and experiments", Doctoral dissertation California Institute of Technology, 1990.
- [9] H. Oloomi, and B. Shafai. "Weight selection in mixed sensitivity robust control for improving the sinusoidal tracking performance." 42nd IEEE International Conference on Decision and Control (IEEE Cat. No. 03CH37475). Vol. 1. IEEE, 2003.
- [10] D.W. Gu, P. Petkov, and M. M. Konstantinov, "Robust control design with MATLAB®", Springer Science & Business Media, 2005.